Supplementary Materials

Characterization of Gas and Particle Emissions from Open Burning of Household Solid Waste

Xiaoliang Wang[1], Hatef Firouzkouhi[1], Judith C. Chow[1], John G. Watson[1], Warren Carter[2], Alexandra S.M. De Vos[2]

[1] Division of Atmospheric Sciences, Desert Research Institute, Reno, NV 89512, U.S.A.
[2] SASOL Research and Technology, Sasolburg, South Africa

Correspondence to: Xiaoliang Wang (xiaoliang.wang@dri.edu)

S1. Supplementary Tables

Table S1: Moisture contents of waste materials.

Material	Moisture (% of dry mass)
Paper	26.5
Leather/Rubber	0.52
Textile	6.9
Plastic bottles	0.54
Plastic bags	0.54
Vegetation	16.5
Food discards	34.7
Combined	8.52

Table S2: Major elemental compositions (mean ± standard deviation of three samples) of waste materials tested in this study and the carbon content assumed for IPCC (2006) emission estimates.

Material	C (%)	H (%)	N (%)	S (%)	O (%)	Other Elements (%)	C% in IPCC (2006)
Paper	44.10 ± 2.82	5.69 ± 0.84	0.68 ± 0.19	0.00 ± 0.00	44.08 ± 0.26	5.45 ± 3.64	46 (42–50)
Leather/Rubber	32.91 ± 0.07	2.88 ± 0.01	0.66 ± 0.00	0.16 ± 0.01	23.64 ± 0.27	39.76 ± 0.52	67
Textile	47.81 ± 3.50	5.84 ± 0.81	7.71 ± 1.11	0.71 ± 0.31	33.62 ± 2.63	4.32 ± 2.39	50 (25–50)
Plastic bottles	63.72 ± 5.36	5.10 ± 0.23	0.41 ± 0.09	0.00 ± 0.00	22.77 ± 2.35	8.00 ± 4.76	75 (67–85)
Plastic bags	84.42 ± 1.80	12.62 ± 0.82	0.20 ± 0.01	0.00 ± 0.00	2.78 ± 0.08	2.76 ± 4.90	
Vegetation	44.60 ± 1.10	5.32 ± 0.87	0.86 ± 0.11	0.00 ± 0.00	42.02 ± 1.65	7.20 ± 2.43	49 (45–55)
Food discards	34.78 ± 2.67	5.51 ± 0.43	3.66 ± 0.09	0.00 ± 0.00	41.43 ± 2.27	14.62 ± 3.68	38 (20–50)
Combined	41.06 ± 0.94	4.62 ± 0.70	1.50 ± 0.14	0.00 ± 0.00	21.32 ± 2.25	31.50 ± 3.50	NA

Table S3: Ash fractions (mass ratio of ash to the original dry materials) and major elemental compositions (mean ± standard deviation of three samples) for tested waste materials.

Material	Ash Fraction (%)	Major Elemental Content			
		C (%)	H (%)	N (%)	S (%)
Paper	6.9 ± 1.6	7.11 ± 0.34	0.22 ± 0.03	0.00 ± 0.00	0.00 ± 0.00
Leather/rubber	58.0 ± 2.3	12.80 ± 0.20	1.07 ± 0.32	0.00 ± 0.00	0.00 ± 0.00
Textile	11.1 ± 1.4	9.14 ± 1.01	0.37 ± 0.01	1.18 ± 0.32	0.00 ± 0.00
Plastic bottles	5.3 ± 3.1	77.44 ± 4.93	2.95 ± 0.30	0.11 ± 0.05	0.00 ± 0.00
Plastic bags	3.4 ± 1.0	10.99 ± 1.39	0.48 ± 0.05	0.21 ± 0.03	0.00 ± 0.00
Vegetation (0% mc*)	8.8 ± 2.6	6.21 ± 1.20	0.50 ± 0.08	0.18 ± 0.02	0.00 ± 0.00
Vegetation (20% mc*)	8.3 ± 0.4				
Vegetation (50% mc*)	7.5 ± 0.0				
Food discard	2.1 ± 0.5	41.04 ± 0.53	1.77 ± 0.04	3.23 ± 0.06	0.00 ± 0.00
Combined	19.9 ± 1.9	2.36 ± 0.93	0.31 ± 0.10	0.04 ± 0.06	0.00 ± 0.00

*mc: fuel moisture content. Elemental compositions for vegetations with 20% and 50% moisture content are assumed to be the same as that with 0% moisture content.

Table S4: Gas and particle measurement instruments for the combustion experiments.

Make/Model	Equipment Type and Operating Principle	Measurement Range	Data Rate
Li-Cor Model 840A CO_2 Analyzer	CO_2 analyzer by non-dispersive infrared (NDIR)	0–20000 ppm	1 s
Thermo 48i CO Analyzer	CO analyzer by gas filter correlation infrared absorbance	0–400 ppm	1 s
Thermo 43i SO_2 Analyzer	SO_2 analyzer by pulsed fluorescence	0–10 ppm	1 s
Testo Model 350 XL Emission Analyzer	CO (electrochemical) CO_2 (nondispersive infrared) NO (electrochemical) NO_2 (electrochemical) SO_2 (electrochemical) O_2 (electrochemical) Temperature Gauge Pressure	0–500 ppm 0–50% vol 0–300 ppm 0–500 ppm 0–5,000 ppm 0–25% vol -40–1200 °C -40–40 hPa	1 s
Horiba Model APNA-360 NO/ NO_2 Analyzer	NO, NO_2, and NO_x by chemiluminescence	0–1 ppm	1 s
TSI Model 8534 DustTrak DRX Aerosol Monitor	PM_1, $PM_{2.5}$, PM_4, PM_{10}, and PM_{15} by light scattering	0–400 mg m^{-3}	1 s
Dekati ELPI+	Particle size distribution	0.006–10 µm	0.1 s
DMT PASS-3 Soot Spectrometer	Light absorption by photoacoustic spectrometry and light scattering by integrated nephelometry at 3 wavelengths: 405, 532, and 781 nm	Absorption (2-s average): 3 Mm^{-1} @781nm, 10 Mm^{-1} (@ 532 and 405 nm	2 s
DRI Multi-Channel Low-volume Filter Sampler	Four filter channels to collect $PM_{2.5}$ for mass and future chemical analysis, as well as one Teflon filter for PM_{10} mass	Flow: 5 L min^{-1} each channel	30–120 min integrated

Table S5: Comparison of measured and calculated emission factors for combined materials.

Combined Materials	Emission Factor (g kg^{-1} fuel)							
	CO_2	CO	NO (as NO_2)	NO_2	NO_x (as NO_2)	SO_2	$PM_{2.5}$	PM_{10}
Measured	1417	31.6	1.80	0.61	2.41	0.95	6.86	7.26
Calculated	1499	48.8	1.8	0.7	2.5	0.6	49.5	53.8
Relative Difference*	6%	54%	0%	8%	2%	-39%	621%	642%

*$Relative\ Difference = (Calculated - Measured)/Measured$

S2. Supplementary Figures

30

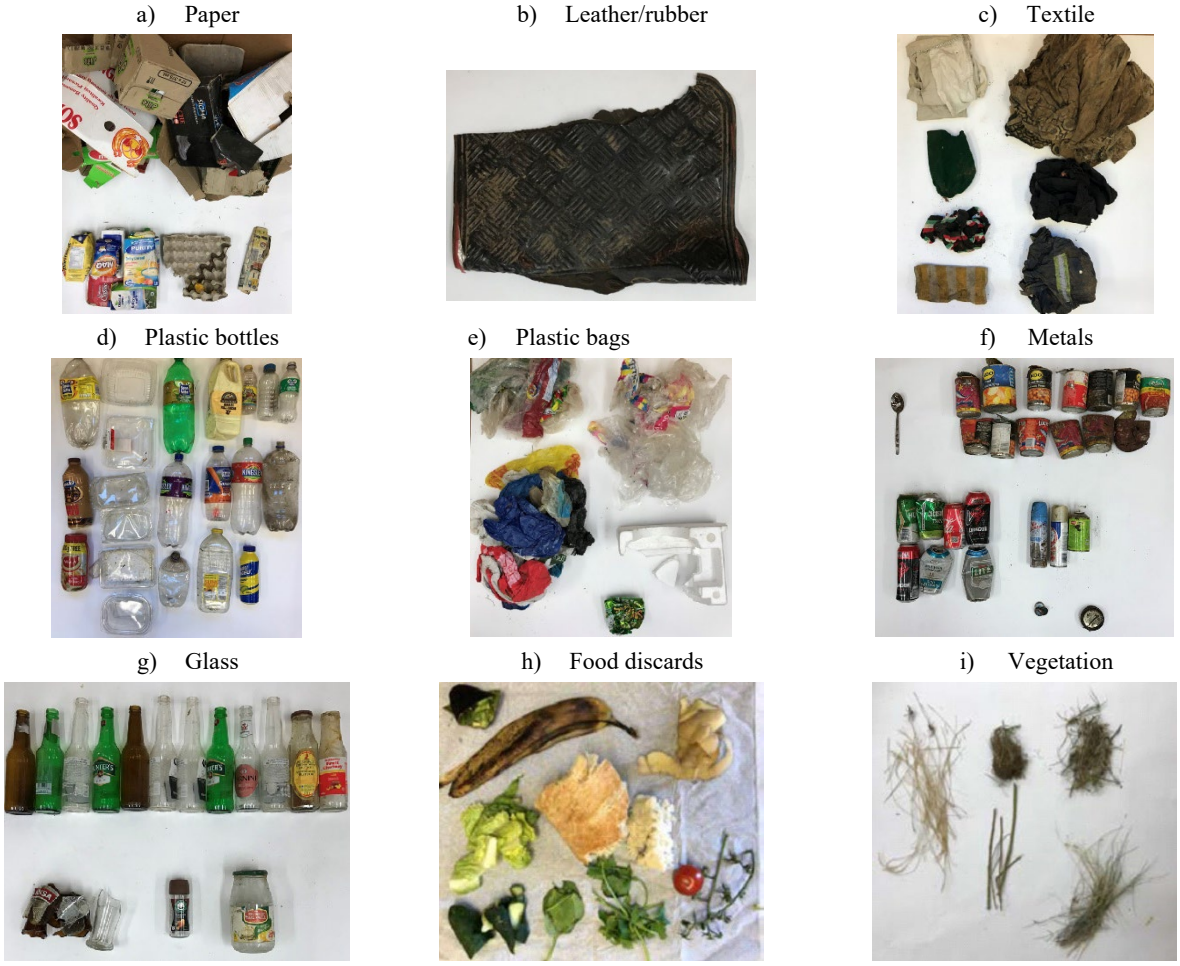

Figure S1: Photographs of household solid waste materials used in this study.

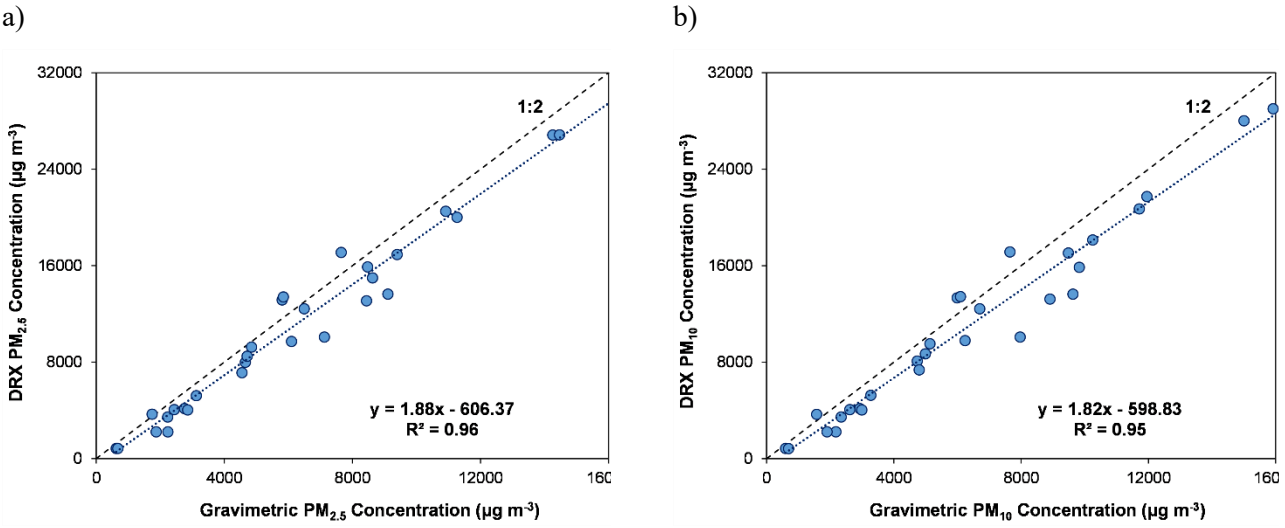

Figure S2: Comparisons of: a) $PM_{2.5}$ and b) PM_{10} mass concentrations by DRX and by gravimetry.

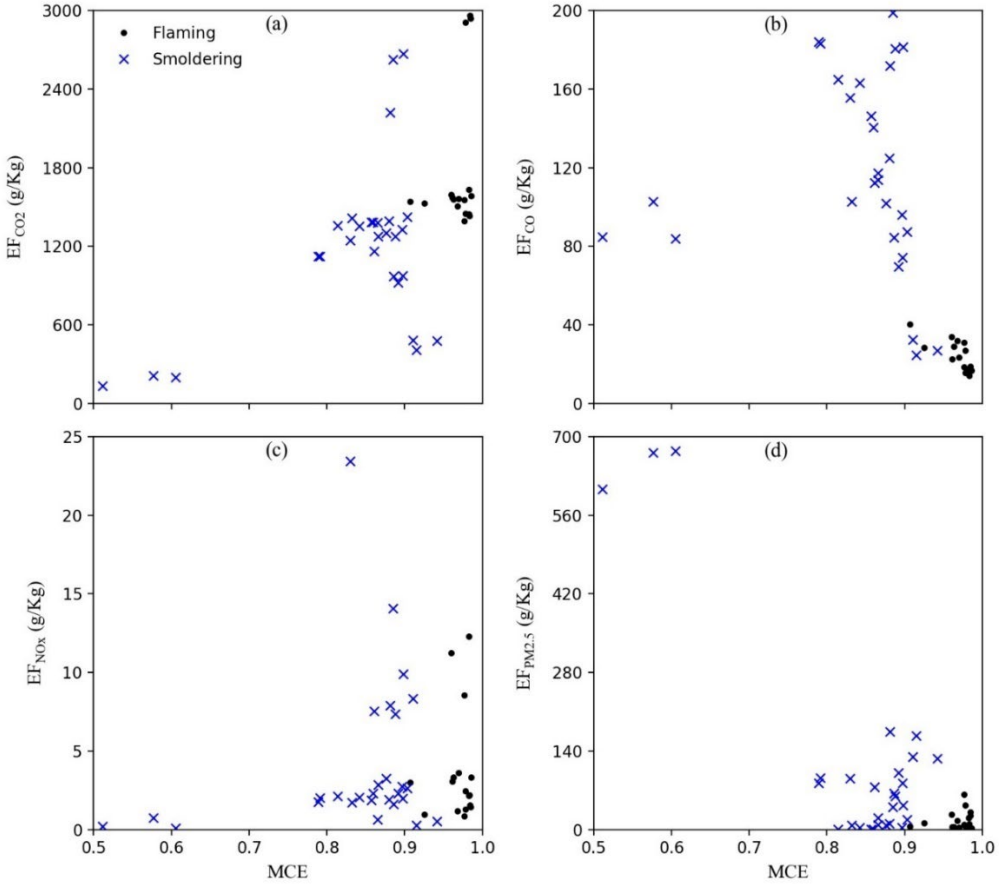

Figure S3: Flaming and smoldering emission factors vs MCE for: (a) CO_2, (b) CO, (c) NO_x (as NO_2), and (d) $PM_{2.5}$ for all fuels.

S3 Air Pollutant Emission Evolution during Combustion

This section presents time series plots of criteria pollutant emissions as a function of time during the burns. Time series plots provide insights into combustion behaviors of different waste materials.

S3.1 Paper

The paper burning experiment utilized 10 g of dried paper, moisturized to 26.5% water content. The prepared material was then placed in a heated ceramic crucible inside the burn chamber and was subjected to exhaust from a heat gun. The material was ignited after ~40 seconds, as indicated by the left boundary of the shaded area in Figure S4, and the paper started flaming with increasing pollutant concentrations. Pollutants related to more complete combustion and higher combustion temperatures (i.e., CO_2, SO_2, NO, and NO_2) increased faster than those related to incomplete combustion (i.e., CO and $PM_{2.5}$). The MCE was high (>0.93). As the paper was consumed, the fire became smaller, and CO_2, SO_2, NO, and NO_2 concentrations decreased. There was also a period when flaming and smoldering emissions coexisted. Eventually, the visible flame died out and smoldering emissions took over (as indicated by the right boundary of the shaded area).

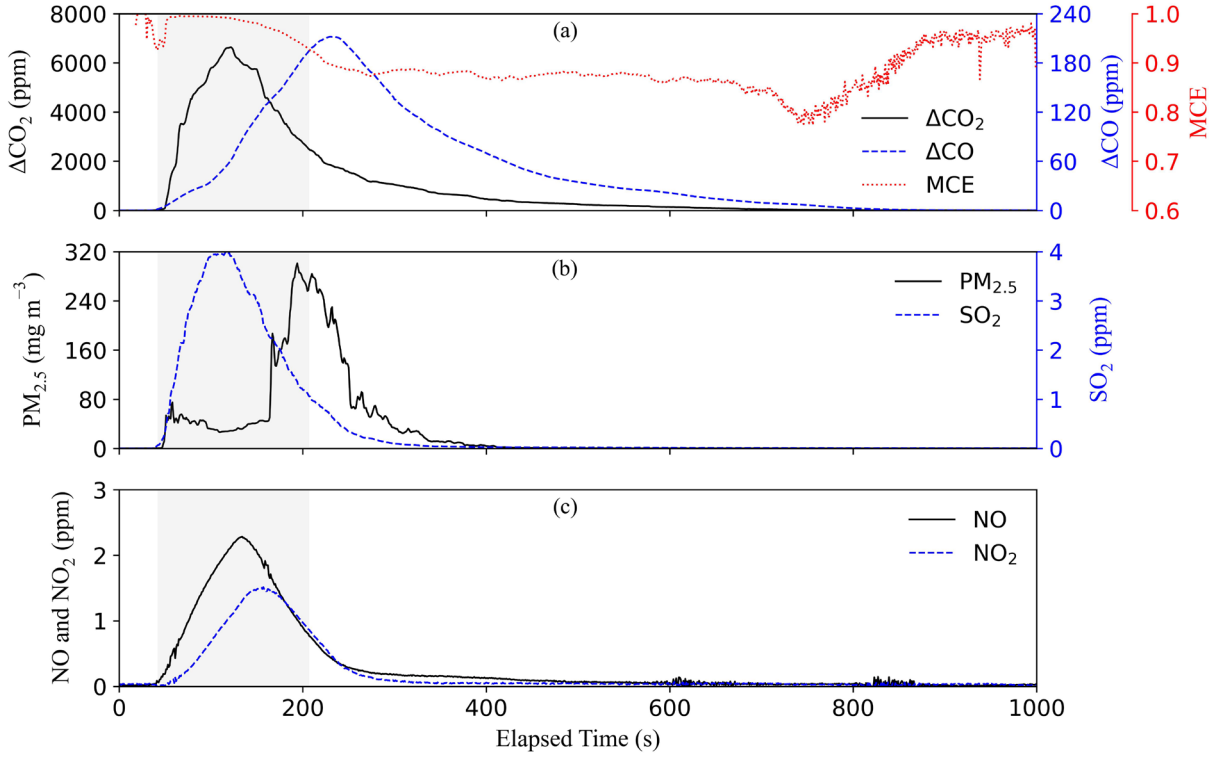

Figure S4: Time series of pollutant concentrations during a paper burning experiment. The shaded area indicates flaming stage.

During smoldering, CO_2, SO_2, NO, and NO_2 continued to decrease while CO and $PM_{2.5}$ concentrations reached their maxima and gradually decreased as the fuel was consumed. The MCE remained low during the smoldering stage. The higher MCE at the end of the experiment (after ~750 seconds) was an artifact due to CO concentrations being near background levels.

The test ended when all concentrations attained background levels. The heater was turned off and filters and ashes were collected for weighting and laboratory analysis. Figure S5 shows the fuel and ashes at the end of the test. Filter deposits from the paper test are shown in Figure S6, with the $PM_{2.5}$ and PM_{10} filters containing 1.69 and 1.78 mg PM mass, respectively. OC and EC were 55.1% and 6.6% of $PM_{2.5}$, respectively. The light yellow color of the filters indicates the presence of brown carbon - light absorbing particles at shorter visible wavelengths.

a) b)

Figure S5: Paper material in a heated- ceramic crucible: a) before burning and b) after burning.

Figure S6: Filters with PM collected from paper burning tests; from left to right: Teflon-membrane for $PM_{2.5}$, two Quartz filters in the middle for $PM_{2.5}$, and Teflon-membrane for PM_{10}.

S3.2 Leather/Rubber

The leather/rubber material was derived from a car floor mat. Unlike tires, this rubber material does not flame, but it pyrolyzes, decays, and evaporates when heated, similar to smoldering for the other fuels. Three grams of chopped rubber material moisturized to 0.52% was placed in the ceramic crucible (Figure S7a). The test started by setting the heater temperature to 450 °C; after ~200 seconds, the fuel reached ~100 °C and smoldering started. As shown in Figure S8, all pollutants gradually increased, except for NO_x that forms at high temperatures. CO and CO_2 concentrations were low – almost the lowest among all tests, while $PM_{2.5}$ concentrations were high. The rubber tests yielded the second highest (after plastic bottles) emission factors for PM. Almost all rubber was consumed after ~26 minutes, and all pollutants returned to background levels. The MCE was ~92% during most part of the smoldering.

By the end of the test, more than half of the fuel remained as ash (Figure S7b). Rubber had the most unburned residue among all tested waste materials (Table S3). This is consistent with the high fraction of elements other than C, H, N, S, and O in Table S2. High amounts of ash (~58%) play an important role in EF calculation according to Eq. (2).

Figure S9 shows the filters from this test, which look like the blank filter. However, each $PM_{2.5}$ and PM_{10} filter contained 2.36 and 2.47 mg PM mass, respectively, indicating the lack of visible light absorbing components, as also evidenced by the low EC (0.2% of $PM_{2.5}$) loadings.

a) b)

Figure S7: Rubber material in a heated ceramic crucible: a) before burning and b) after burning.

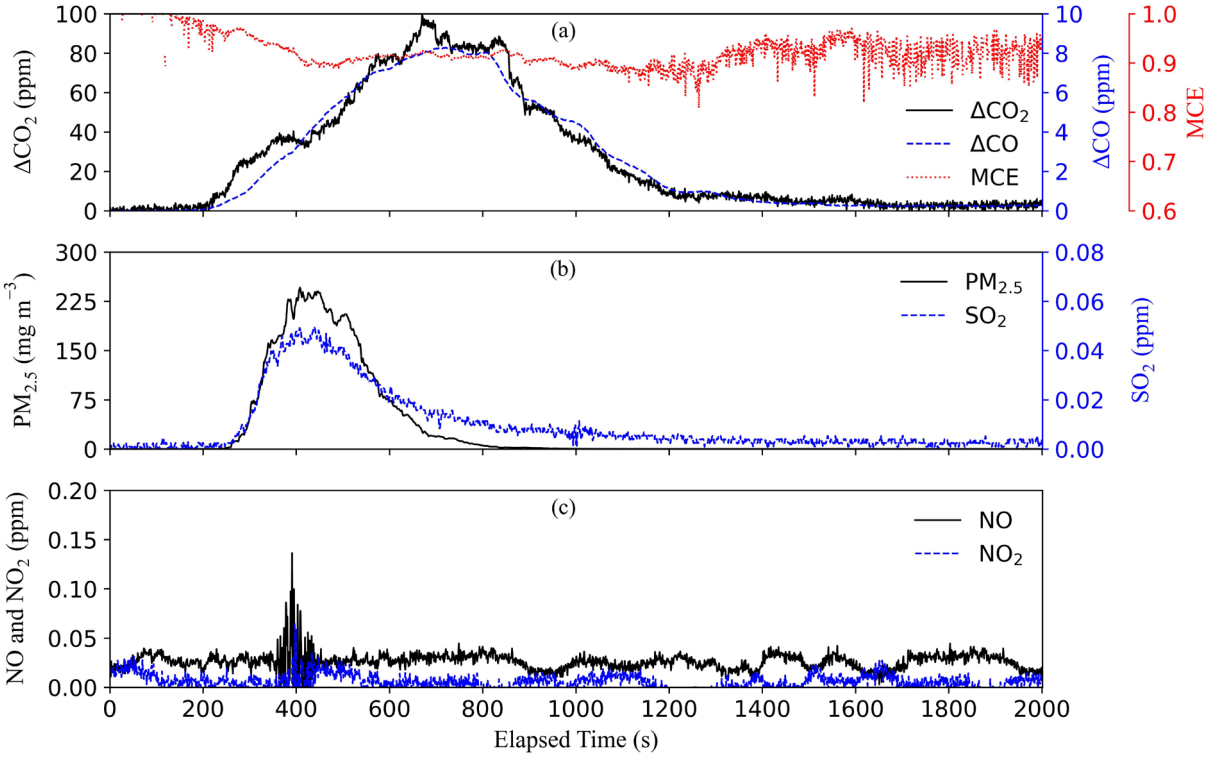

Figure S8: Concentration time series during a rubber burning experiment.

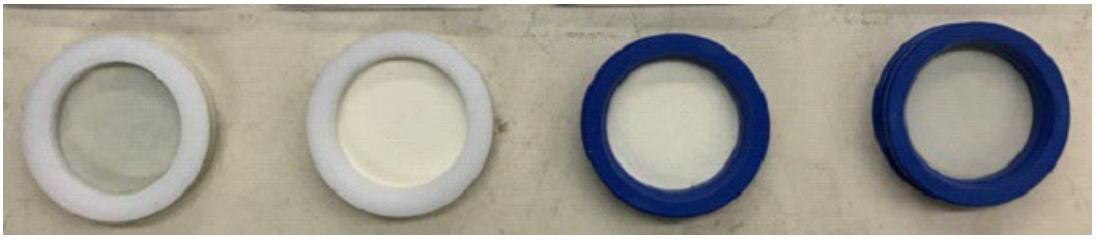

Figure S9: Filters with PM collected from rubber burning tests; from left to right: Teflon-membrane for $PM_{2.5}$, two Quartz filters in the middle for $PM_{2.5}$, and Teflon-membrane for PM_{10}.

S3.3 Textiles

Figure S10a shows 5 g of the prepared textile material that was moisturized to 6.9% water content. Combustion showed two flaming stages caused by the different textile types in the fuel mix. One part of the fuel started to flame right after ignition by the heat gun (first shaded area). After the more flammable materials were consumed, the fire smoldered for ~140s, then the less flammable materials started to flame (second shaded area). Although the first flaming stage had higher CO_2, SO_2, and NO_x emissions, the second flaming phase had higher CO and PM emissions. The mean MCE for the second flaming stage was lower than that for the first one. Among all tested materials, the textiles had the highest emission factors for NO_x and SO_2.

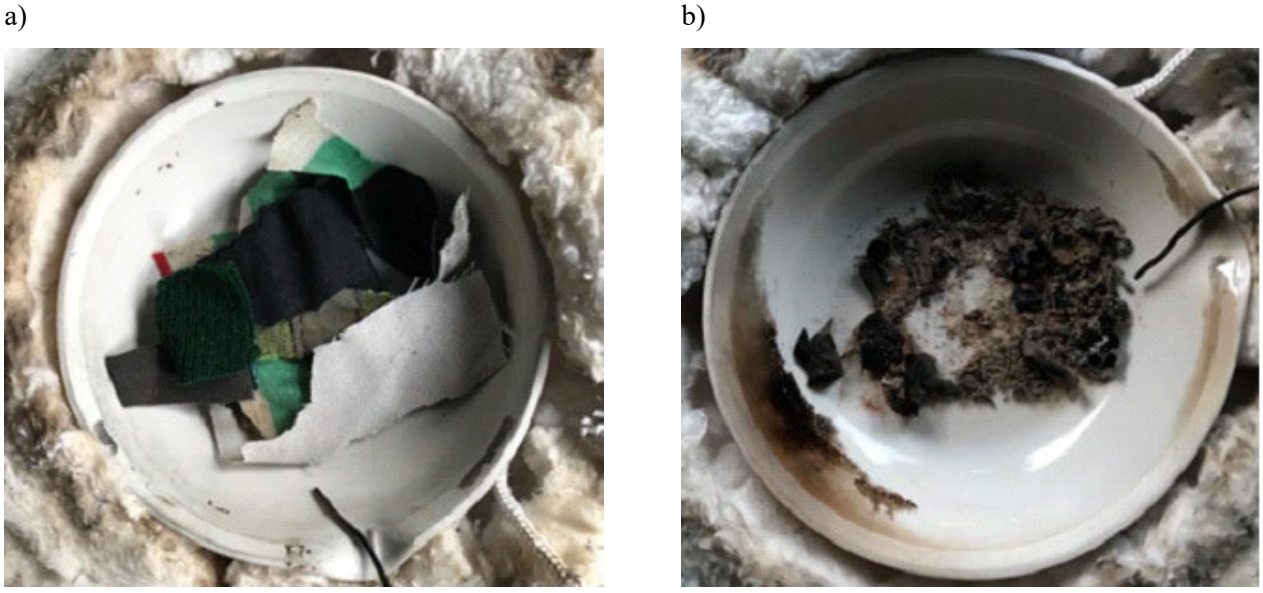

Figure S10: Textile material in a heated ceramic crucible: a) before burning and b) after burning.

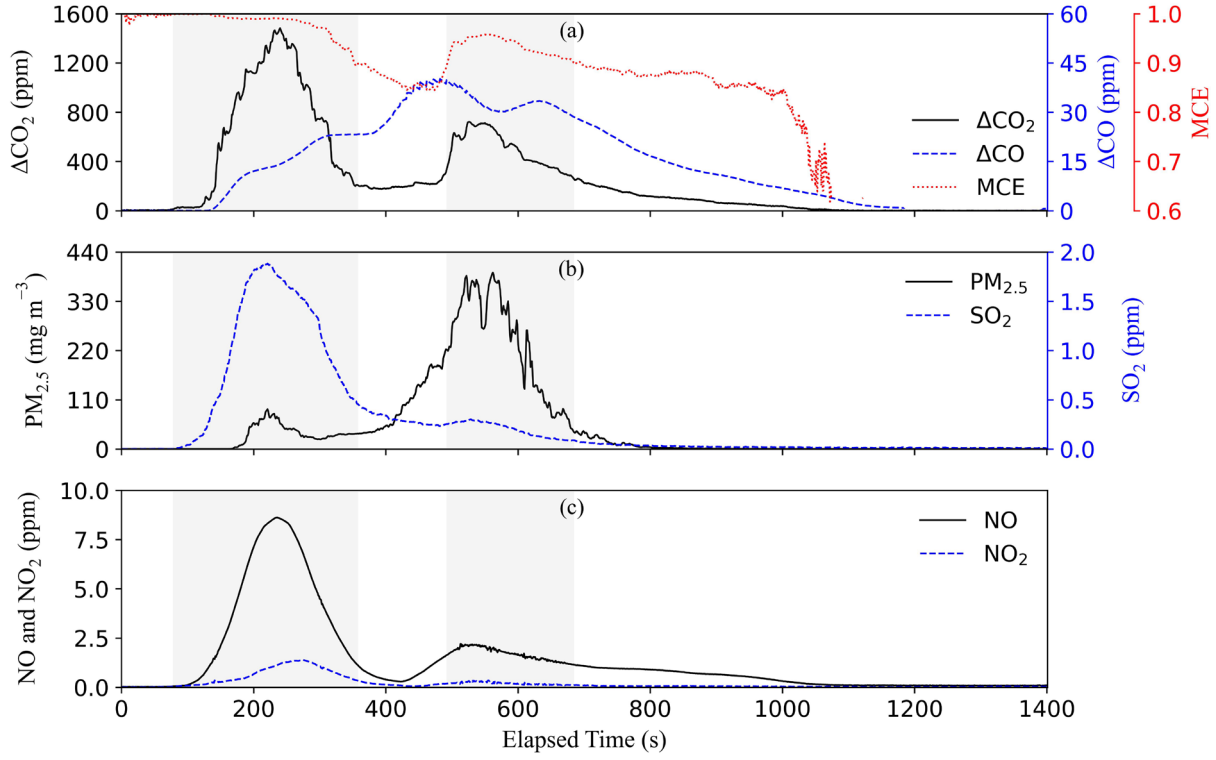

Figure S11: Time series of concentrations during a textile burning experiment. The shaded areas indicate flaming stages.

Textile ash, Figure S10b, was ~11% of the fuel total weight. The collected filters are depicted in Figure S12, with each $PM_{2.5}$ and PM_{10} filter containing 1.16 and 1.18 mg of PM mass, respectively. The PM deposits were dark grey, consistent with abundant EC levels (15% of $PM_{2.5}$). The dark color of indicates that the textile smoke has a significant light absorption effect.

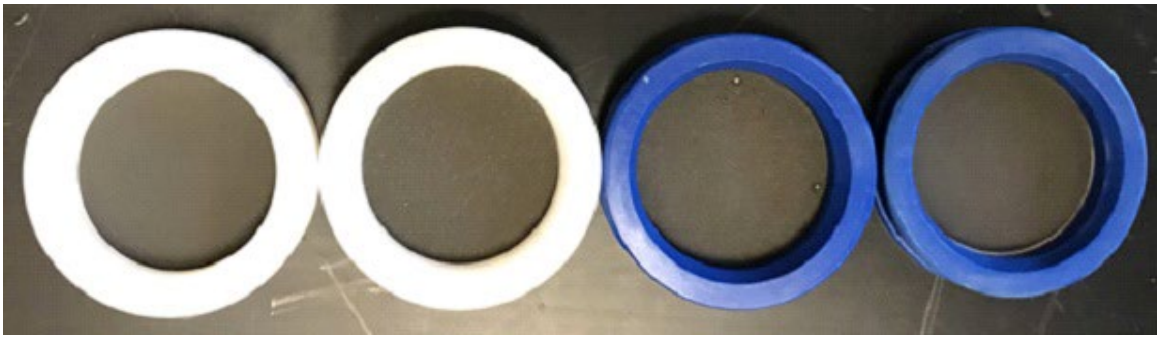

Figure S12: Filters with PM collected from a textile burning; from left to right: Teflon-membrane for $PM_{2.5}$, two Quartz filters in the middle for $PM_{2.5}$, and Teflon-membrane for PM_{10}.

S3.4. Hard Plastic (Bottles)

Smoldering combustion of plastic bottles (hard plastic) generated high PM concentrations that clogged filters and contaminated some test instruments during initial trial burns. Only 0.5 g of the prepared material, as shown in Figure S13a, was used for subsequent burns. The moisture content of the plastic bottles was 0.54%.

a) b)

Figure S13: Hard plastic (bottle) material in a heated ceramic crucible: a) before burning and b) after burning.

Concentration time series plots are shown in Figure S14. The bottles did not flame and only smoldered, generating low CO_2 and CO emissions. However, PM emissions were the highest among all the waste materials. The strong plastic odor and light-yellow colored sticky particles were likely formed from re-condensation of evaporated plastic molecules. The MCE was only ~0.6 during most of the burn, indicating low combustion efficiencies. The low combustion temperature and low nitrogen content in the fuel (Table S2) resulted in low NO_x emissions.

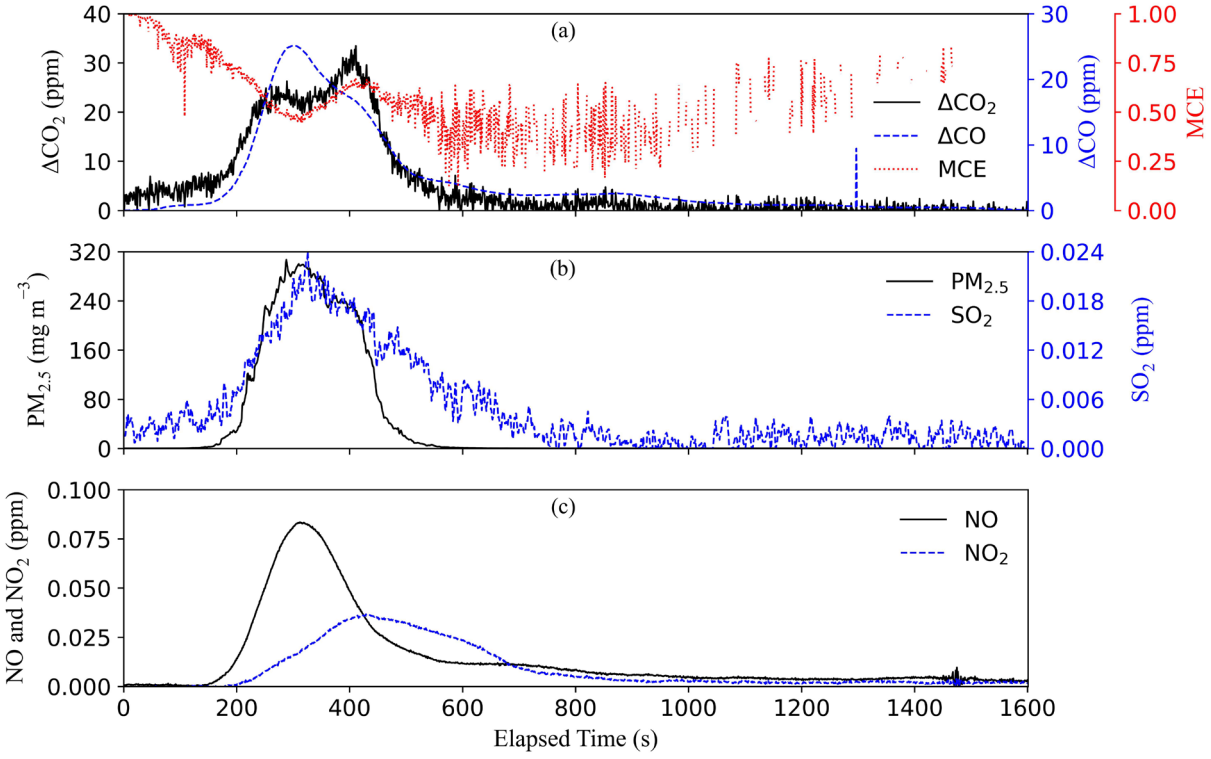

Figure S14: Time series of concentrations during a hard plastic (bottles) burning experiment.

Almost all of the fuel was consumed, and only ~5% ash remained as illustrated in Figure S13b. Strong smoldering was observed when the heater temperature exceeded 350 ˚C. The PM deposit appearances (Figure S15) were similar to those of blank filters, although $PM_{2.5}$ and PM_{10} filters contained 2.49 and 2.72 mg PM mass, respectively, indicating the smoke was mainly composed of non-light absorbing PM composition at visible wavelengths with low amounts of elemental carbon (<1% of $PM_{2.5}$).

Figure S15: Filters with PM collected from hard plastic (bottle) burning; from left to right: Teflon-membrane for $PM_{2.5}$, two Quartz filters in the middle for $PM_{2.5}$, and Teflon-membrane for PM_{10}.

S3.5 Soft Plastic (Bags)

Soft plastic materials - mostly composed of shopping bags, packaging bags, bubble wrap, and cellophanes - form a large portion of the household wastes. Plastic waste is the second most common part of South African municipal solid waste (Fig. 1). It is estimated that plastic materials production and will double in next 20 years. Plastics are mostly used in packaging or construction (Lebreton and Andrady, 2019). In this test, 5 g of the material shown in Figure S16a was prepared with 0.54% moisture content.

In contrast to the smoldering-only combustion of hard plastic (bottles), flaming dominated soft plastic combustion (Figure S17). The MCE was high (> 0.94) during most parts of burn, indicating high combustion efficiencies. Soft plastic bags had the highest and lowest emission factors for CO_2 and CO, respectively, consistent with their high C and H contents (Table S2). A small amount of ash (3.4%) remained in the crucible (Figure S16b). PM deposits on filters were black (Figure S18) - the darkest among all samples, with $PM_{2.5}$ and PM_{10} filters containing 1.51 and 1.59 mg PM mass, respectively. These emissions had the highest EC abundances (70% of $PM_{2.5}$).

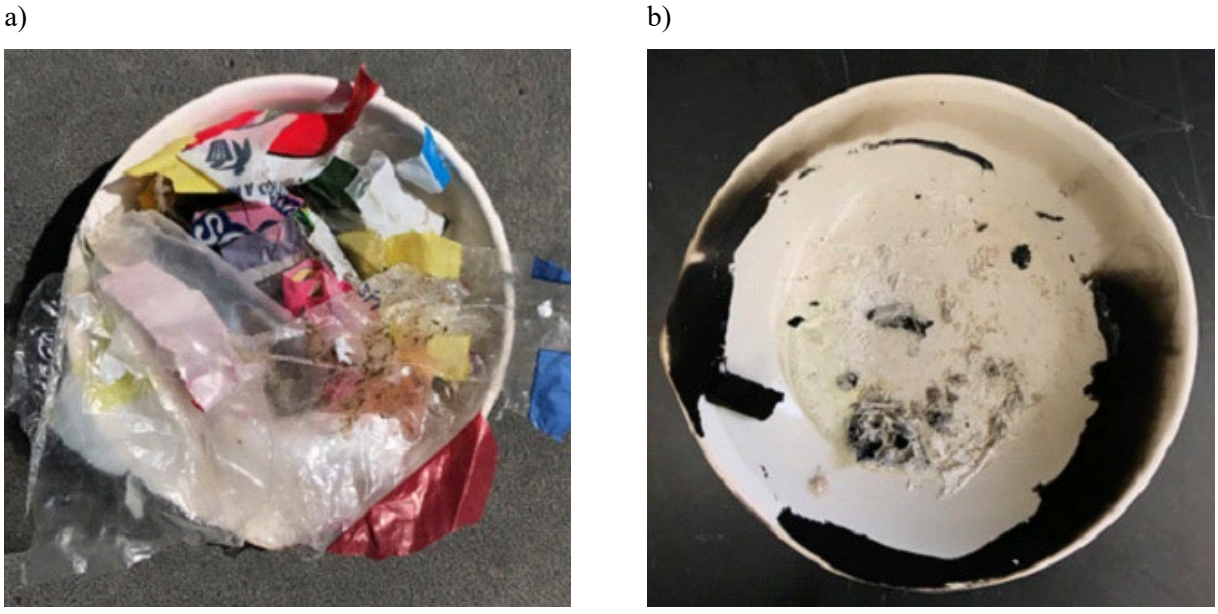

Figure S16: Soft plastic (bags) material in a heated ceramic crucible: a) before burning and b) after burning.

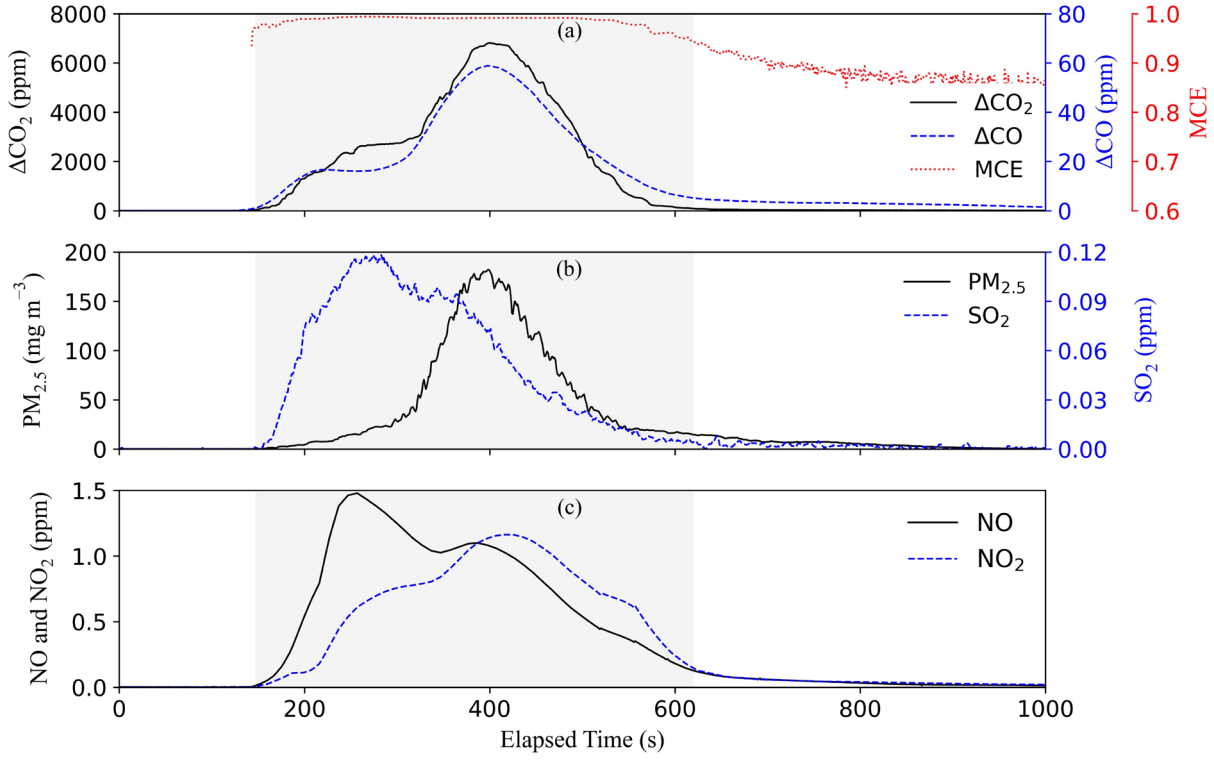

Figure S17: Time series of emissions during a soft plastic (bags) burning experiment. The shaded area indicates flaming stage.

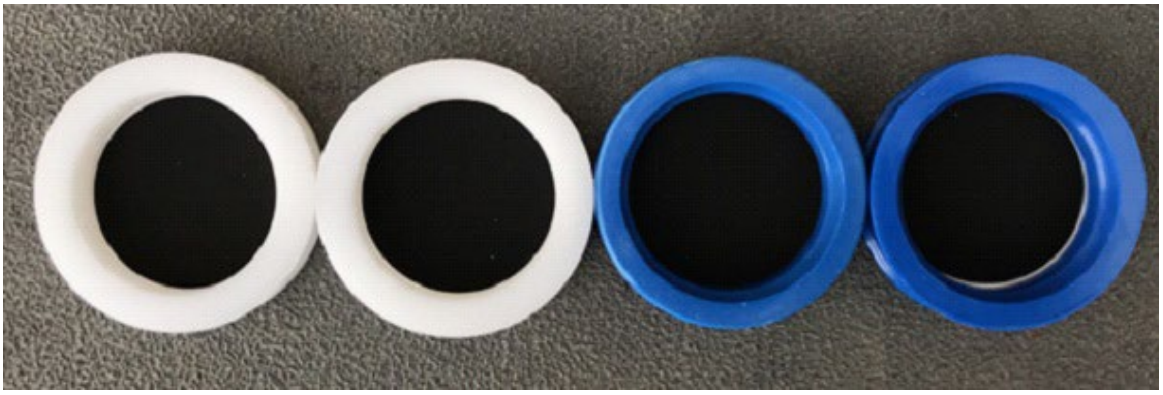

Figure S18: Filters with PM collected from a soft plastic (bags) burning test; from left to right: Teflon-membrane for $PM_{2.5}$, two Quartz filters in the middle for $PM_{2.5}$, and Teflon-membrane for PM_{10}.

S3.6 Wood / Vegetation

For the vegetation burns, 10 g of the dry vegetation, 10 g with 20% moisture, and 2 g with 50% moisture contents were prepared (Figure S19). Figure S20, Figure S21, and Figure S22 show pollutant concentration time series for the different moisture contents. Burning behaviors between the 0% and 20% moisture contents were similar, except that the flaming started earlier for the 20% moisture content case (indicated by a smaller peak at the beginning of the test). Once the moisture evaporated upon heating, most of the fuel was consumed by flaming. The combustion behavior for the 50% moist vegetation was different. The fuel only smoldered, probably owing to water evaporation during heating; the fuel charred and did not flame. The damp vegetation emitted less CO_2, but higher levels of CO and PM. Different emission factors observed between vegetations with 50% and 0-20% moisture contents underline the importance of and also the challenges in obtaining representative fuel conditions for accurate real-world pollutant emissions. The MCEs for 0%, 20%, and 50% moisture content vegetation were ~0.92, ~0.9, and 0.8, respectively, indicating the role of the moisture in the combustion efficiency (Chen et al., 2010). At the end of the test, 7.5 to 8.8% of the fuel weight (Table S3) remained as ash, indicating that most of the fuel participated in the burn.

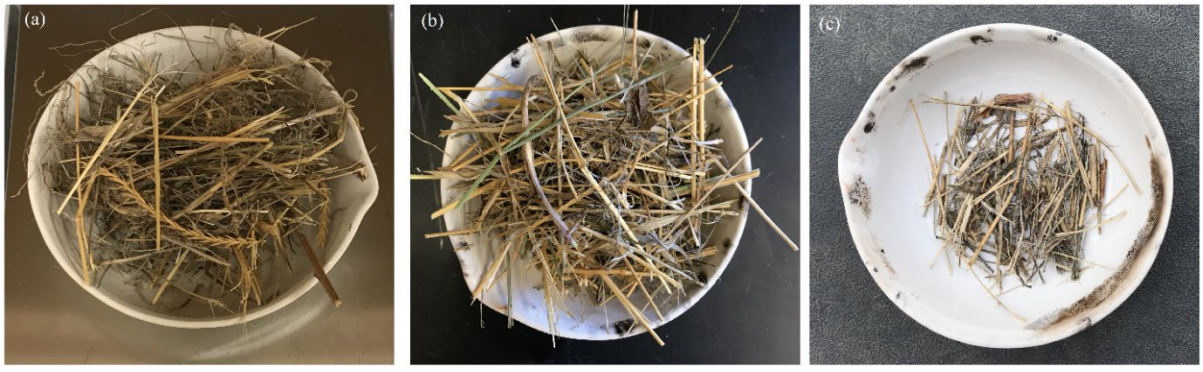

Figure S19: Vegetation material, in a heated ceramic crucible for: (a) dry, (b) 20%, and (c) 50% moisture content.

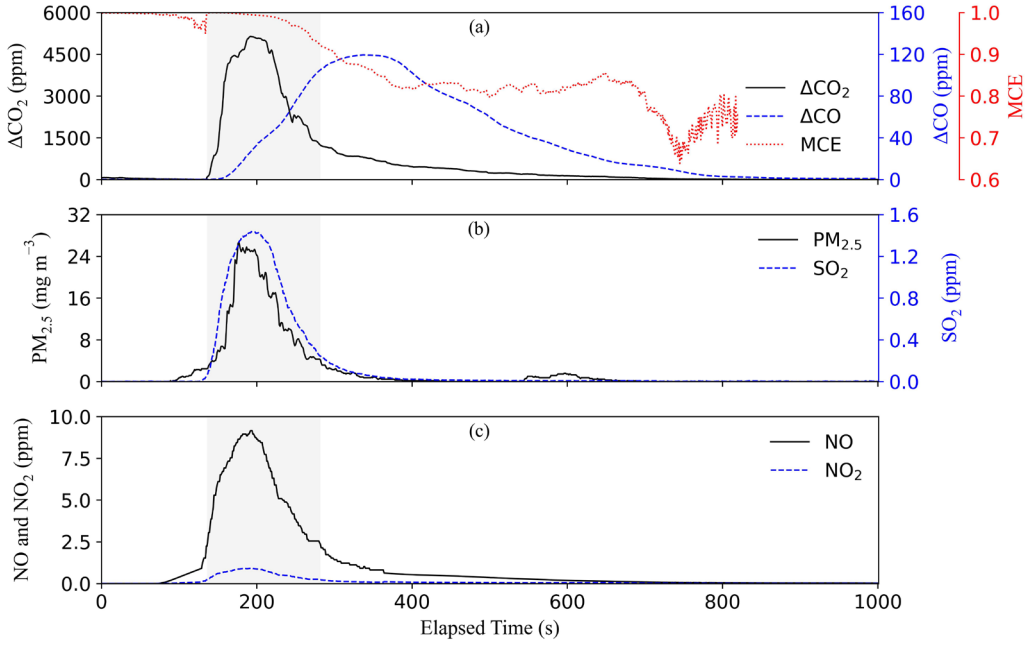

Figure S20: Time series of concentrations during a dry vegetation (0% moisture) burning experiment. The shaded area indicates the flaming stage.

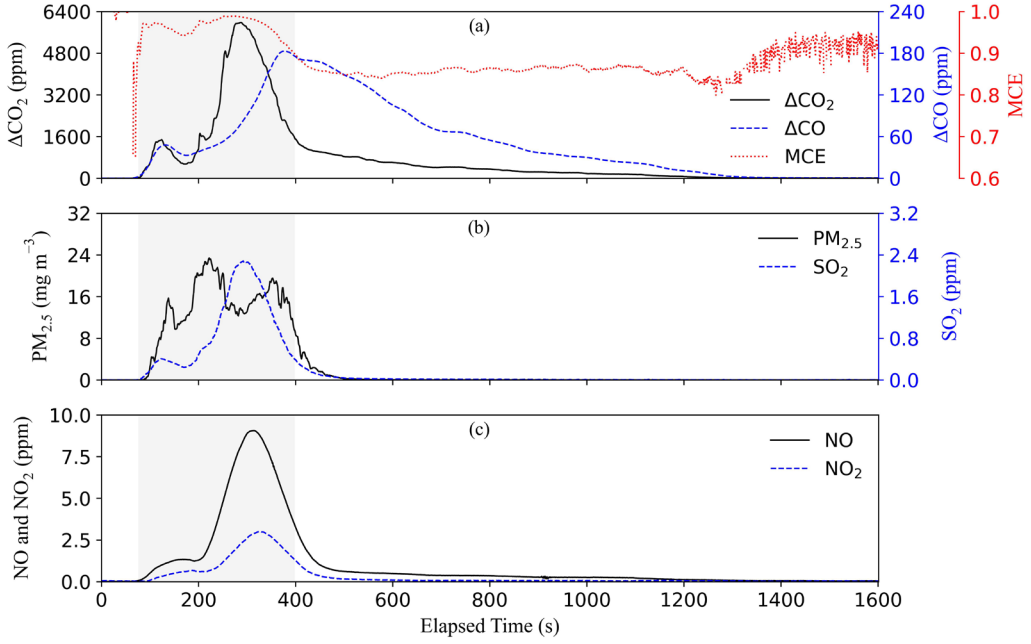

Figure S21: Time series of concentrations during a vegetation (20% moisture) burning experiment. The shaded area indicates flaming stage.

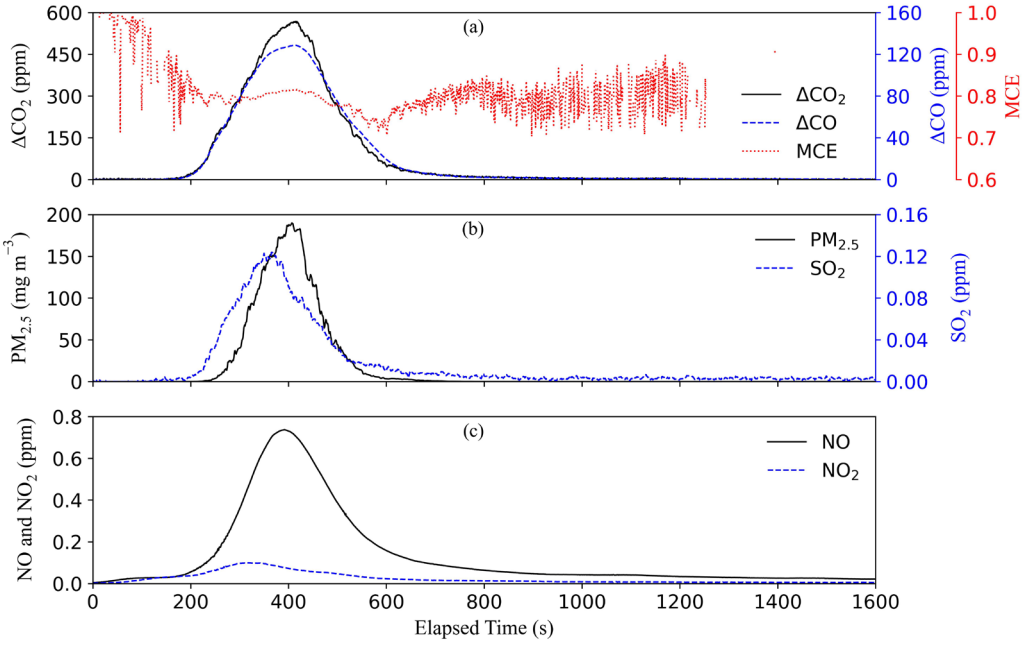

Figure S22: Time series of concentrations during a vegetation (50% moisture) burning experiment.

Figure S23: Vegetation ashes for: (a) dry, (b) 20%, and (c) 50% moisture contents.

Sampling filters from emissions of the vegetation with 0 and 20% moisture often look like blank filters; however, the 50% moisture fuel gave a pale yellow color (Figure S24). The $PM_{2.5}$ and PM_{10} filter mass loadings are: 0.12 and 0.12 mg for dry fuel, 0.32 and 0.33 mg for 20% moist fuel, and 1.19 and 1.25 mg for 50% moist fuel, respectively. The EC abundance decreased from 9.3% of $PM_{2.5}$ for dry fuel, to 4.4% of $PM_{2.5}$ for 20% moist fuel, and to 2.7% of $PM_{2.5}$ for 50% moist fuel due to decreasing flaming and increasing smoldering as moisture content increased. Filters from the 50% moist fuel show a pale yellow color, indicating the presence of more brown carbon components in the smoldering smoke of this fuel.

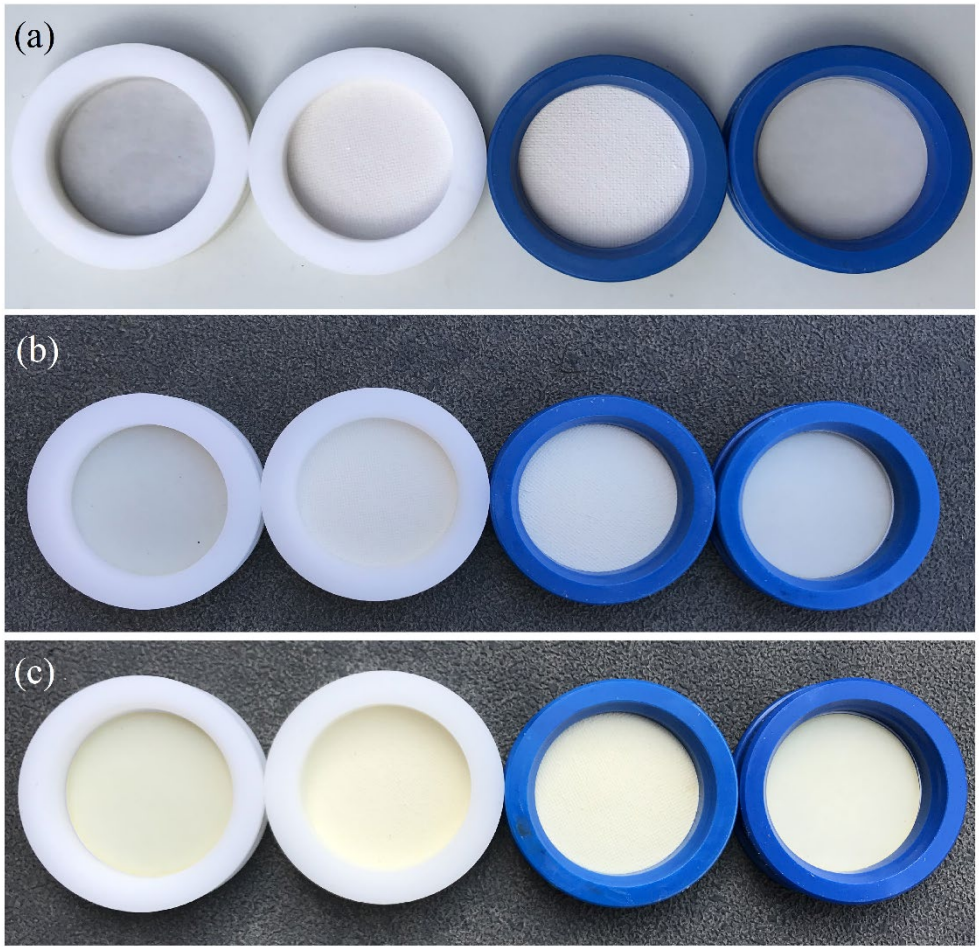

Figure S24: Filters with PM collected from three vegetation burning tests. (a): dry, (b): 20%, and (c): 50% water content; from left to right: Teflon-membrane for $PM_{2.5}$, two Quartz filters in the middle for $PM_{2.5}$, and Teflon-membrane for PM_{10}.

S3.7 Food Discards

As shown in Figure S25a, food waste was represented by a mixture of bread, potato and banana peels, lettuce, cucumber, and tomato (Cronjé et al., 2018). In their natural state, food discards had a moisture content of 34.7% (Table S1), the highest among all tested waste materials. The time series for burning of food discards are shown in Figure S26. Only smoldering was observed due to high moisture content, with low CO_2 and high CO and PM emissions. The MCE was ~0.90 during the most parts of the burn.

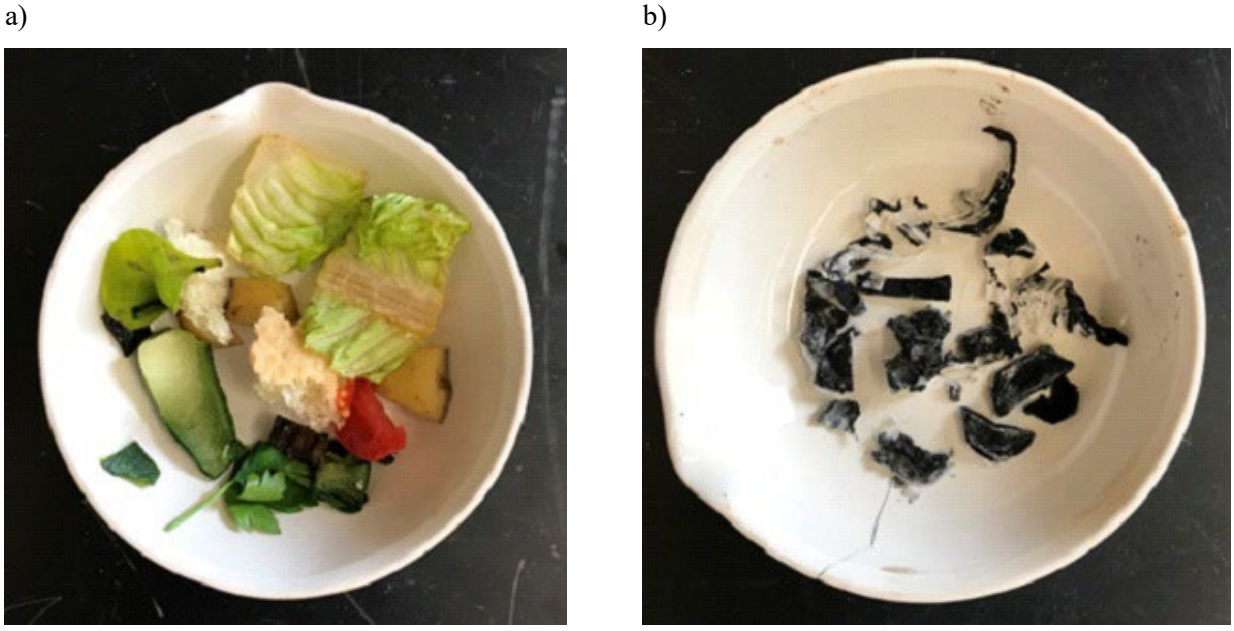

Figure S25: Food discard materials in a heated ceramic crucible: a) before burning and b) after burning.

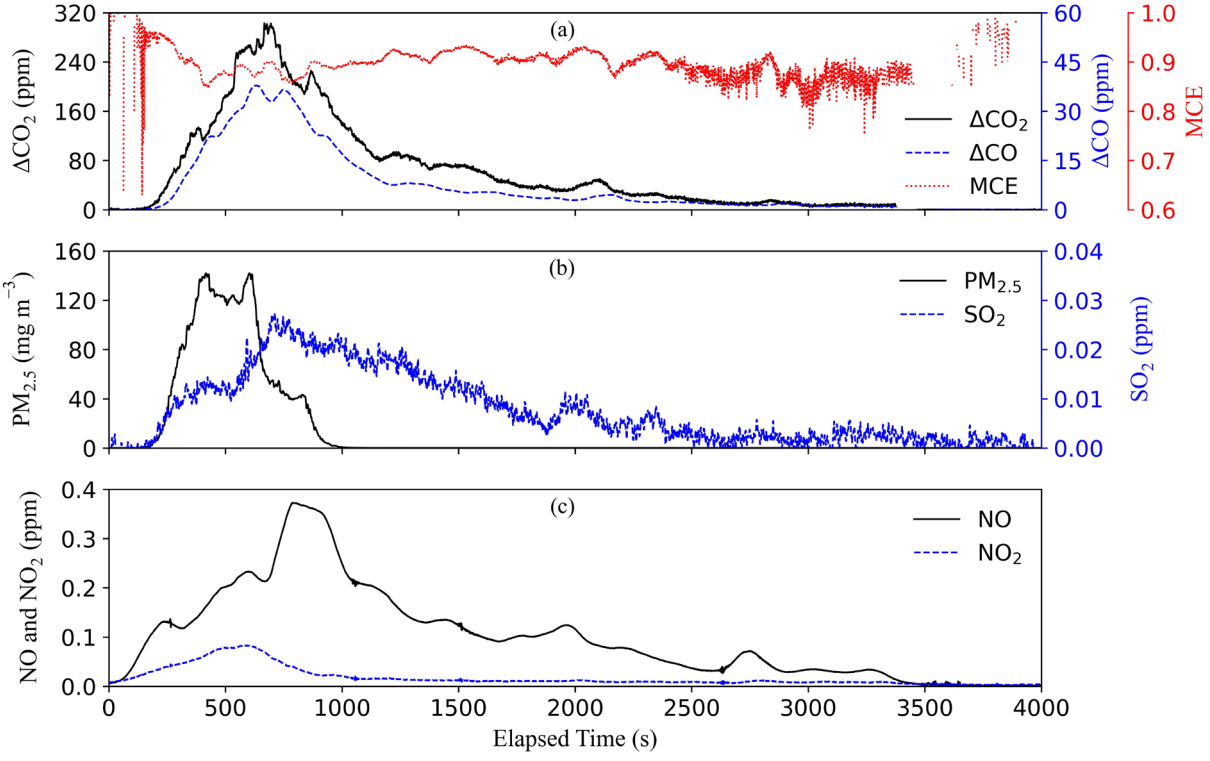

Figure S26. Time series of concentrations during a food discards burning experiment.

Due to their organic nature, food discards only had ~2% dry mass remaining as ash (Figure S25b) after combustion, the lowest ash fraction among the fuels (Table S3). PM deposits on the filters are depicted in Figure S27, with the $PM_{2.5}$ and PM_{10} filters containing 2.27 and 2.31 mg PM mass, respectively. OC and EC were 52.5% and 0.8% of $PM_{2.5}$, respectively. The yellow appearance of the filters indicates the presence of brown carbon compounds that absorb light at shorter visible wavelengths.

Figure S27: Filters with PM collected from food discards burning; from left to right: Teflon-membrane for $PM_{2.5}$, two Quartz filters in the middle for $PM_{2.5}$, and Teflon-membrane for PM_{10}.

S3.8 Combined Materials

The final tests involved a mixture from all waste categories, including ceramic, glass, and metals. Although ceramic, glass, and metal were not combustible at typical open burning temperatures, they were included to evaluate real-world combustion of a mixed waste stream. Based on the weight fraction of materials in the combined group (Fig. 1), 10 g of the fuel with 8.52% moisture content was prepared, as shown in Figure S28a.

The combustion behavior of combined waste materials (Figure S29) was similar to those of paper (Figure S4) and dry vegetation (Figure S20). Flaming was initiated in the most flammable materials such as paper and plastic bags, causing increased pollutant releases related to more complete combustion and higher combustion temperatures (i.e., CO_2, SO_2, NO, and NO_2). Peak concentrations of CO and PM appeared when the combustion transitioned from flaming to smoldering. The MCE for most of the burn period exceeded 0.90. After >5 minutes, the visible flame died out followed by the smoldering phase.

Figure S28b shows that about 2 g (20% of dry mass) ash remained in the crucible; considering that glass, metal and ceramic did not contribute to the combustion, a high ash fraction was expected. PM deposits are illustrated in Figure S30, with the $PM_{2.5}$ and PM_{10} filters containing 0.67 and 0.70 mg PM mass, respectively. The black color of the filters is due to abundant EC (48.1% of $PM_{2.5}$ mass), which has high light absorption efficiency for all wavelengths.

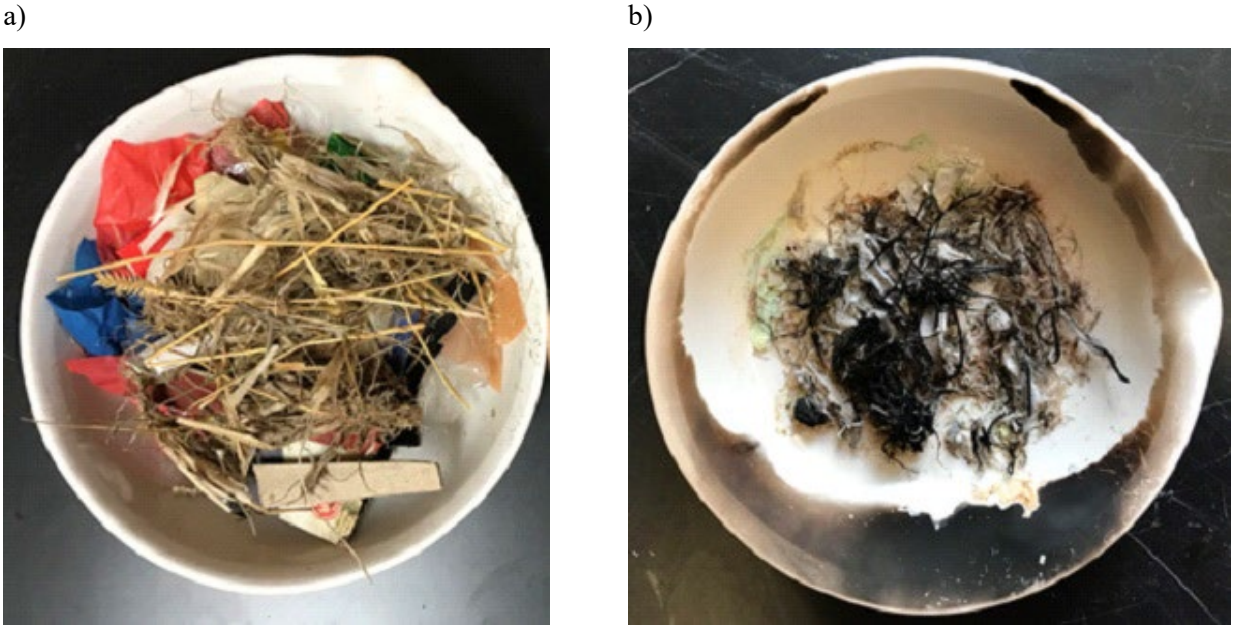

Figure S28: Combined materials in a heated ceramic crucible: a) before burning and b) after burning.

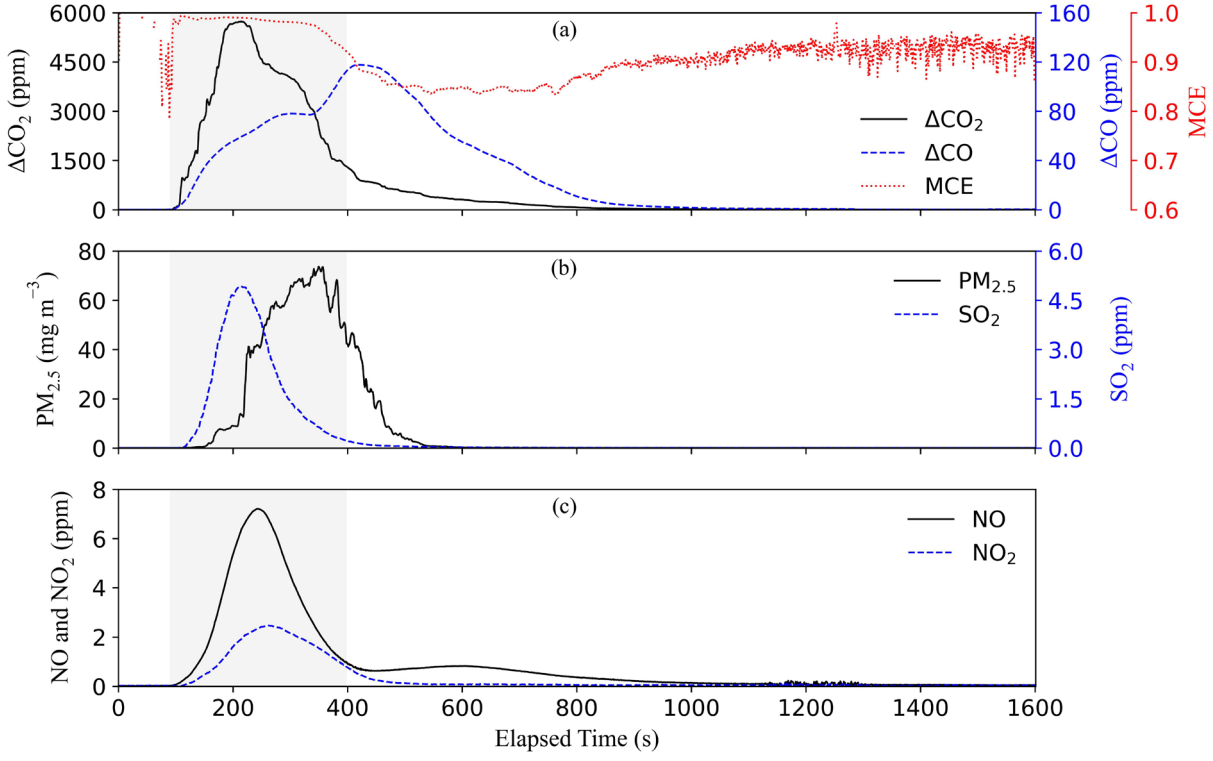

Figure S29: Time series of concentrations during combined waste burning experiment. The shaded area indicates flaming stage.

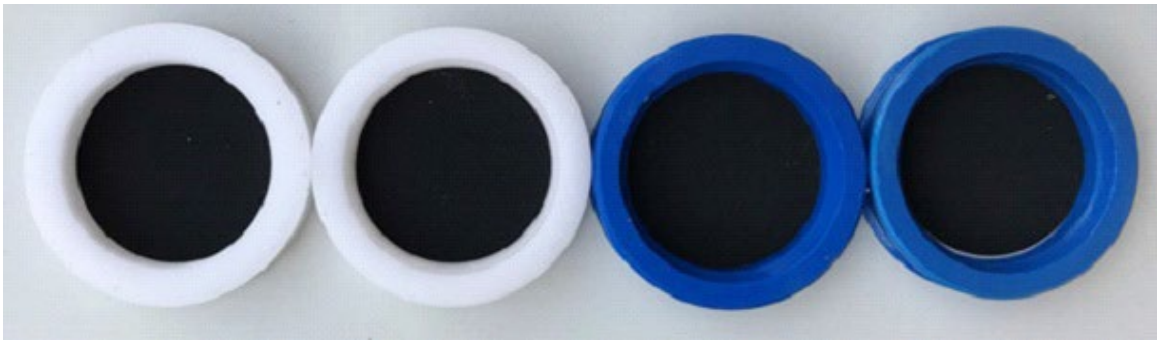

Figure S30: Filters with PM collected from a combined materials burning test; from left to right: Teflon-membrane for $PM_{2.5}$, two Quartz filters in the middle for $PM_{2.5}$, and Teflon-membrane for PM_{10}.